Preprints.org

Article

N-Acetylcysteine-Amide Protects Against Acute Acrylamide Neurotoxicity in Adult Zebrafish

Niki Tagkalidou , Júlia Goyenechea-Cunillera , Irene Romero-Alfano , Maria Olivella Martí ,

Juliette Bedrossiantz , Eva Prats , Cristian Gomez-Canela , Demetrio Raldúa [*]

Article

N-Acetylcysteine-Amide Protects Against Acute Acrylamide Neurotoxicity in Adult Zebrafish

Niki Tagkalidou [1], Júlia Goyenechea-Cunillera [2], Irene Romero-Alfano [2], Maria Olivella Martí [2], Juliette Bedrossiantz [1], Eva Prats [3], Cristian Gomez-Canela [2] and Demetrio Raldúa [1,*]

[1] Institute for Environmental Assessment and Water Research (IDAEA-CSIC), Jordi Girona, 18, 08034 Barcelona, Spain; niki.tagkalidou@idaea.csic.es (N.T.); jbdqam@cid.csic.es (J.B.)

[2] Department of Analytical and Applied Chemistry, School of Engineering, Institut Químic de Sarrià-Universitat Ramon Llull, Via Augusta 390, 08017 Barcelona, Spain; juliagoyenecheac@iqs.url.edu (J.G.-C.); ireneromeroa@iqs.url.edu (I.R.-A.); mariaolivellam@iqs-blanquerna.url.edu (M.O.M.); cristian.gomez@iqs.url.edu (C.G.-C.)

[3] Research and Development Center (CID-CSIC), Jordi Girona, 18, 08034 Barcelona, Spain; eva.prats@cid.csic.es (E.P.)

* Correspondence: drpqam@cid.csic.es

Abstract: Acrylamide (ACR) is a potent neurotoxicant that disrupts cellular redox homeostasis by depleting reduced glutathione (GSH) and inducing oxidative stress. Despite its well-characterized mechanism, effective treatments for ACR-induced neurotoxicity remain elusive. This study evaluates the therapeutic potential of N-acetylcysteine-amide (AD4), a blood-brain barrier-permeable derivative of N-acetylcysteine, in a novel severe acute ACR neurotoxicity model in adult zebrafish. Intraperitoneal administration of a single high dose of ACR (800 mg/kg) resulted in a 51% reduction in brain GSH levels, which was fully rescued by AD4 treatment. Behavioral analyses revealed that ACR exposure impaired short-term habituation of the acoustic startle response (ASR), a deficit that was mitigated by AD4. Surprisingly, ACR exposure did not alter the neurochemical profile of key neurotransmitters or the expression of genes related to redox homeostasis, synaptic vesicle recycling, regeneration, or myelination. These findings highlight the efficacy of AD4 in counteracting ACR-induced oxidative stress and behavioral deficits, underscoring its potential as a therapeutic agent for ACR neurotoxicity. This study also validates the adult zebrafish as a translational model to investigate neurotoxic mechanisms and evaluate neuroprotective interventions.

Keywords: acrylamide; neurotoxicity; zebrafish model; glutathione; acoustic startle response; habituation; kinematic analysis

1. Introduction

Acrylamide (ACR) is a water-soluble type-2 alkene widely used in industrial applications [1,2]. It is known for its mutagenic, carcinogenic, and neurotoxic properties [3]. In humans, ACR exposure typically leads to peripheral neuropathy, characterized by ataxia, skeletal muscle weakness, and sensory deficits in the extremities [4–6]. The neurotoxic effects of ACR are primarily attributed to its ability to form adducts with specific proteins critical for maintaining neural homeostasis [7]. For instance, we and others have provided evidence demonstrating that ACR can form adducts with free thiol groups on key components of the antioxidant defense system, such as reduced glutathione (GSH) and thioredoxin, disrupting the cellular redox state by increasing the levels of reactive oxygen species (ROS) [7–9].

Zebrafish (Danio rerio) has emerged as a powerful vertebrate model for studying neurotoxicity due to its conserved nervous system architecture and neurotransmitter pathways, which closely resemble those of mammals [10,11]. Both larval and adult zebrafish exhibit neurotoxic responses to

ACR exposure, including molecular and behavioral alterations comparable to those observed in mammalian models [9,12–14]. While larvae offer high-throughput screening capabilities, adult zebrafish provide a more translationally relevant system for studying complex neurobehavioral outcomes due to their fully developed central nervous system and diverse behavioral repertoire [15].

Despite extensive research into the mechanisms of ACR neurotoxicity, effective treatments are still lacking. Current management is mainly symptomatic, and even mild cases of ACR poisoning often result in incomplete recovery [4]. Given that ACR toxicity involves oxidative stress and GSH depletion, antioxidant-based therapeutic strategies have been explored [16]. N-acetylcysteine (NAC), a precursor of L-cysteine and glutathione, has been investigated as a potential treatment due to its ability to replenish intracellular GSH levels and scavenge electrophilic toxicants. However, despite its effectiveness against ACR neurotoxicity in in vitro models, NAC has shown limited success in protecting against ACR-induced neurotoxicity, largely due to its poor blood-brain barrier (BBB) permeability [14,16,17]. N-acetylcysteine amide (NAC-amide or AD4), a modified derivative of NAC with enhanced lipophilicity, was recently developed as a promising neuroprotective agent able to cross BBB [18,19]. Given its improved pharmacokinetic profile, AD4 represents a compelling candidate for mitigating ACR-induced neurotoxicity [16].

In this study, we developed a severe acute ACR neurotoxicity model in adult zebrafish to evaluate the therapeutic efficacy of AD4. Using a combination of behavioral, biochemical, and molecular approaches, we demonstrate that AD4 fully rescues ACR-induced GSH depletion and mitigates behavioral deficits, highlighting its potential as a therapeutic agent for ACR neurotoxicity.

2. Materials and Methods

2.1. Chemicals

Acrylamide (CAS 79-06-1) was purchased at Sigma-Aldrich (St. Louis, MO, USA; A9099-25G, purity 100%). N-acetylcysteine-amide (NAC-amide or AD4; CAS 38520-57-9) was a kind gift from Dr. Daphne Atlas, at Hebrew University of Jerusalem. Prior to the start of the experiment ACR and AD4 were dissolved in phosphate-buffered saline (PBS) at concentrations 80 mg/mL and 40 mg/mL, respectively.

2.2. Fish Husbandry

Adult zebrafish (0.41 ± 0.1 g) were sourced from Pisciber (Barcelona, Spain) and acclimated at the Research and Development Center (CID-CSIC) for a period of two months before the start of the experiments. The fish were housed in a recirculating zebrafish system (Aquaneering Inc., San Diego, USA) under controlled conditions. They were kept in 2.8 L tanks filled with fish water, consisting of reverse-osmosis purified water supplemented with 90 mg/L Instant Ocean® (Aquarium Systems, Sarrebourg, France), along with 0.58 mM $CaSO_4 \cdot 2H_2O$ and 0.59 mM $NaHCO_3$. Environmental parameters were maintained at 28 ± 1°C with a 12-hour light/12-hour dark photoperiod. The zebrafish were fed twice daily with dried food (TetraMin, Tetra, Germany).

2.3. Experimental Design

All procedures were conducted in compliance with the institutional guidelines and were approved by the Institutional Animal Care and Use Committees at CID-CSIC (OH 1432/2023), with authorization from the local government (agreement number 9820). The study adhered to the ARRIVE guidelines for reporting animal research [20]. For intraperitoneal (i.p.) injections, zebrafish were randomly selected from breeding tanks (0.38-0.45 g; ≈50:50 male:female ratio) and anesthetized via hypothermia. Fish were positioned dorsoventrally, and each individual received an injection of 10 µL of solution per gram of body weight into the peritoneal cavity using a 10 µL glass Hamilton syringe equipped with an ultrafine needle [21].

Three experimental groups were set (see Figure 1). Control group received a 1st i.p. injection of PBS at time 0 and a 2nd i.p. injection of PBS at 24h. ACR group received a 1st i.p. injection of 800 mg/kg of ACR at time 0 and a 2nd i.p. injection of PBS at 24 h. Finally, AD4 group received a 1st i.p. injection of 800 mg/kg of ACR at time 0 and a 2nd i.p. injection of 400 mg/kg of AD4 at 24 h.
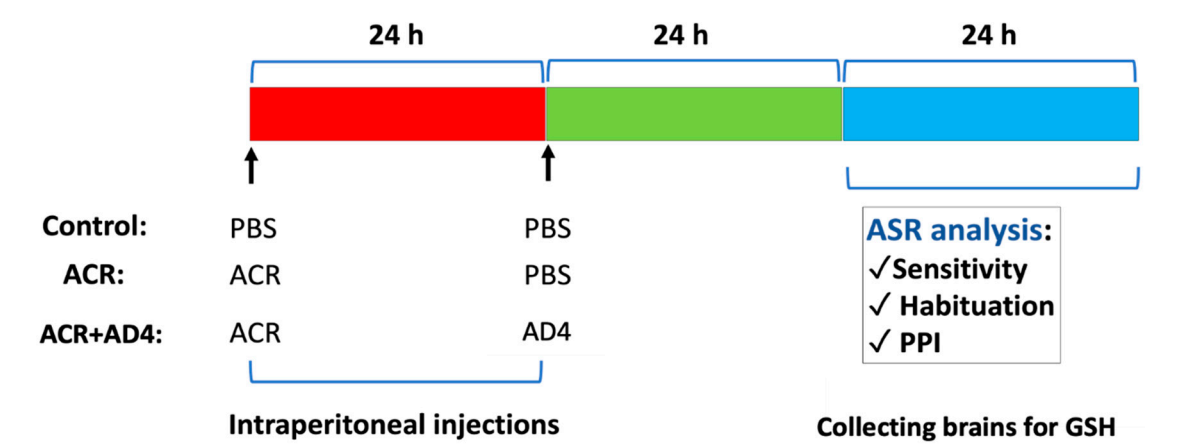

Figure 1. Experimental design of the new acute ACR neurotoxicity model developed in adult zebrafish.

Throughout the study, zebrafish were housed in 2.8 L tanks, provided with food, and maintained in a climate-controlled room at 28°C under a 12-hour light/12-hour dark cycle. Water changes were performed daily. At the end of the experimental period, fish were euthanized by hypothermic shock in ice-cold water. Brains were dissected 48 h after the first injection and stored at -80°C for subsequent analyses.

2.4. GSH Determination

The quantification of reduced glutathione (GSH) was performed using a fluorescence-based microplate assay, adapted from White et al. (2003) [22]. This method detects GSH by measuring the fluorescence emitted upon its conjugation with naphthalene dicarboxaldehyde (NDA). Briefly, zebrafish brains were weighed before homogenization in ice-cold TES/SB buffer (20 mM Tris, 250 mM sucrose, 1 mM EDTA, 20 mM sodium borate, 2 mM serine, pH 7.4) at a ratio of 16.5 mg/ml. The homogenates were centrifuged at 12,000 × g for 10 min at 4°C, and the supernatants were collected for enzyme activity assays and protein quantification. An aliquot of the supernatant (100 μL), referred to as the extract sample, was used for baseline GSH measurement. To inhibit glutamate-cysteine ligase (GCL) activity and precipitate proteins, the extract was diluted threefold by adding equal volumes (100 μL each) of TES/SB buffer and ice-cold 200 mM sulfosalicylic acid (SSA). The mixture was incubated on ice for 10 min to facilitate protein precipitation, followed by centrifugation at 2,500 × g for 5 min at 4°C.

For fluorescence measurement, 20 μL of the resulting supernatant was transferred in triplicate to a black microplate. The extract was further diluted 2.25-fold (resulting in a total dilution of 6.75-fold) with 50 mM Tris-HCl buffer (pH 10). Next, 155 μL of an NDA alkaline solution (50 mM Tris buffer, pH 10; 0.5 N NaOH; 10 mM NDA in DMSO; v/v/v, 7:1:1) was added to each well. The plate was incubated at room temperature for 30 min in the dark. Fluorescence intensity of the GS-NDA cyclic compound was measured using a Synergy 2 Multi-Mode Microplate Reader (BioTek Instruments, Vermont, USA) with excitation and emission wavelengths of 485 nm and 535 nm, respectively. GSH concentrations were determined using a standard curve, and results were expressed as nmol of GSH formed per minute per milligram of tissue.

2.5. Neurotransmitters Assessment

Neurotransmitters, their precursors, and degradation products were extracted from adult zebrafish brains following the methodology outlined in Mayol-Cabré et al. [23]. Briefly, brain samples

were homogenized using a TissueLyser LT (Quiagen, Hilden, Germany), and the resulting supernatant was subjected to centrifugation. The final extract was filtered through a 0.22 μm nylon filter before being transferred directly into chromatographic vials for analysis.

To ensure accurate quantification, an internal standard mixture was added to all samples, allowing for calibration via an internal standard curve. Additionally, quality control (QC) samples were prepared by spiking extracts with a native standard mixture at a concentration of 5 ppm for the target compounds. These QCs were used to assess the efficiency and reliability of the extraction procedure.

The extraction process required high-purity solvents, including HPLC-MS-grade acetonitrile (VWR Chemicals, Leuven, Belgium), LC-MS/MS-grade formic acid (Fisher Scientific, Loughborough, UK), and ammonium formate (Sigma-Aldrich, St. Louis, MO, USA). Ultra-pure water was freshly generated using a Millipore Milli-Q purification system (Millipore, Bedford, MA, USA).

Neurochemical analyses were carried out using UHPLC-MS/MS. Analyte separation and elution were performed on a BEH Amide column, while detection was conducted in multiple reaction monitoring (MRM) mode with electrospray ionization in positive mode (ESI+), ensuring high specificity in both detection and quantification.

Quantification was performed using a reference standard mixture containing acetylcholine, tryptophan, 5-hydroxytryptophan (5-HTP), serotonin, 5-hydroxyindole acetic acid (5-HIAA), tyrosine, L-3,4-dihydroxyphenylalanine (L-DOPA), dopamine, 3,4-dihydroxyphenylacetic acid (DOPAC), 3-methoxytyramine (3-MT), norepinephrine (NE), normetanephrine, and epinephrine, all obtained from Sigma-Aldrich (Steinheim, Germany). In addition, an internal standard mixture was used for further quantification, comprising DL-norepinephrine-d6 (NE-d6), 3-methoxytyramine-d4 hydrochloride (3-MT-d4), and dopamine-1,1,2,2-d4 hydrochloride (DA-d4). These internal standards were sourced from Sigma-Aldrich and Toronto Research Chemicals (TRC, Toronto, Canada).

2.6. Gene Expression Analysis

Total RNA was isolated from whole brains of adult zebrafish from the control, ACR or ACR+AD4 groups sampled 48 hours after ACR injection, using Trizol Reagent (Invitrogen Life Technologies, Carlsbad, CA), following previously described protocols [24]. RNA concentration was measured using a NanoDrop™ ND-8000 spectrophotometer (Thermo Fisher Scientific, Waltham, MA, USA). To remove genomic DNA contamination, samples underwent DNase I treatment (Ambion, Austin, TX), after which first-strand cDNA synthesis was performed using 1 μg of total RNA, the First Strand cDNA Synthesis Kit (Roche Diagnostics, Mannheim, Germany), and oligo(dT) primers, according to the manufacturer's instructions.

Quantitative real-time PCR (qRT-PCR) was carried out using a LightCycler® 480 Real-Time PCR System with SYBR Green PCR Master Mix (Roche Diagnostics, Mannheim, Germany) to validate differential gene expression. The thermal cycling conditions consisted of an initial denaturation step at 95°C for 15 minutes, followed by 45 amplification cycles of 95°C for 10 seconds and 60°C for 30 seconds.

Each experimental group included nine biological replicates, with three technical replicates per sample. Selection of target genes was based in our previous results on transcriptome analysis after ACR exposure, including genes related with redox homeostasis (*gsr*, *gclc*, *txn*), recycling of synaptic vesicles (*nsf1a*, *syn2a*, *syt1a*, *syt2a*, *stxbp1b*), regeneration-associated genes (*gap43*, *gfap*, *tubb5*) and myelination (*mbp*). The expression of these 12 genes was analyzed alongside the geometric mean of the values for the reference genes 2-peptidylprolyl isomerase A (*ppiaa*) and elongation factor 1a (*elf1a*), with primer sequences provided in Supplementary Table S1. Prior to analysis, primer efficiencies and specificities were verified. Relative mRNA abundance was calculated using the ΔΔCt method [25], with fold-change values derived accordingly.

2.7. Kinematic Analysis of the Acoustic Startle Response

Kinematic analyses were conducted in a controlled environment (28°C, darkness) between 10:00 and 17:00. Prior to testing, all zebrafish underwent a one-hour acclimation period in the behavioral testing room.

The kinematic parameters of the acoustic startle response (ASR) in adult zebrafish were evaluated using the Zebra_K platform, as previously described [26]. Additionally, the impact of ACR on sensorimotor gating was assessed through pre-pulse inhibition (PPI) analysis using the same platform. High-speed recordings (115 ms, 1000 fps) were obtained simultaneously from nine experimental arenas using a Photron Fastcam Mini UX100 camera (Photron Ltd., Tokyo, Japan). Video analyses provided key kinematic parameters of the initial C-bend, including latency, duration (time from latency onset to the maximum body curvature), curvature (difference between peak curvature during the C-bend and initial curvature at latency onset), and maximal angular velocity.

The short-term habituation study protocol, adapted from the methodology described by Wolman et al. (2011) [27] for zebrafish larvae, consists of four distinct phases. Initially, in the sensitivity phase, adult subjects were presented with five audiovisual (AV) stimuli of moderate-intensity at 120-second intervals, typically triggering startle responses in 15–30% of cases. Next, during the prehabituation phase, five AV stimuli capable of eliciting startle responses were administered at the same interval. This was followed by the habituation phase, involving 15 consecutive startle-inducing AV stimuli delivered at 1-second intervals. This phase is further divided into early (stimuli 1-5), intermediate (stimuli 6-10) and late (stimuli 11-15) habituation. After a rest period of 300-seconds, the recovery phase commenced, during which five additional startle-inducing AV stimuli were presented every 120 seconds. The level of habituation was determined by comparing the average startle responses from the final five stimuli of the habituation phase with those from the prehabituation phase [27].

For PPI assessment, a low-intensity stimulus (1000 Hz, 10 μs, 72.9 dB re 20 μPa) that typically triggers a 0–10% startle response was used as the prepulse, while a stronger stimulus (1000 Hz, 1 ms, 103.9 dB re 20 μPa) was applied as the startle-inducing pulse. The stimulation protocol consisted of three phases: five prepulse-only stimuli (interstimulus interval [ISI]: 120 s), followed by five pulse-only stimuli (ISI: 120 s), and finally, five combined "prepulse + pulse" sequences (ISI: 120 s). To examine the effect of temporal spacing, two different prepulse-to-pulse intervals (0.5 and 1 s) were tested. PPI percentages were calculated as previously described [28].

2.8. Data Analysis

Statistical analysis was performed using GraphPad Prizm v5 (Graph Pad Software, USA). Normality of the data was assessed using Shapiro-Wilk test. Descriptive statistics were presented as mean ± standard error (SEM) for parametric data, and as median and interquartile range (IQR) for non-parametric data. Data from locomotor activity (total distance travelled) and kinematic studies (latency, duration, curvature and maximal angular velocity) were analyzed using unpaired *t*-test or Mann-Whitney test, with regard to the results of normality distribution. Significance was set at *P*<0.05.

3. Results

3.1. Identification of a Single Dose of Acrylamide Inducing Brain GSH Depletion

The first step in this study was to develop a new severe acute neurotoxicity model induced by ACR in adult zebrafish, based in intraperitoneal administration of this neurotoxicant in a single high dose. Therefore, a range finding test was conducted, injecting fish with 400, 600, 800 and 1000 mg ACR/kg body weight (b.w.), and brains were collected 24 h after injection. As shown in Supplementary Figure S1A, the highest decrease in brain GSH levels, about 70%, was found 24 h after injection with 800 mg/kg without further enhancing the effect on GSH depletion. The effect of a single

i.p. injection on brain GSH levels was further confirmed in a new experiment with a larger sample size (Supplementary Figure S1B). Therefore, a single dose of 800 mg ACR/kg b.w. (11.25 mM) was used to build the new model.

3.2. AD4 Fully Counteracts the Depletion of GSH Stores in the Brain Led by ACR Exposure

Figure 1 summarizes the experimental design used in this study. Using this model we found that 48 h after the ACR injection, GSH levels in the brain were $51.46 \pm 3.01\%$ of the control values [$N_{control}$=33, N_{ACR} = 32 (5 independent experiments); $t(63)$ = 14.014, P = 4.99 x 10^{-21}]. AD4 [400 µg/g b.w. (2.50 mM)], administered intraperitoneally 24 h after ACR-injection, was able to fully counteract the ACR-induced depletion of brain GSH stores (Figure 2, Supplementary Dataset 1). While GSH in the brains of ACR-injected fish decreased to $49.19 \pm 3.38\%$ (n= 26) of controls, administration of AD4 24 h after ACR injection led to a full recovery, with brain GSH levels $101.38 \pm 2.85\%$ (n=23) of the control ($F(2,73)$ = 113.548, P = 3.90 x 10-23). GSH levels in the brain of the ACR-treated fish were significantly lower than those of control and ACR+AD4 treated fish (ACR vs Control, P = 5.10 x 10^{-9}; ACR vs ACR+AD4, P = 5.10 x 10^{-9}; Control vs ACR+AD4, P = 0.937; one-way ANOVA with Tukey's multiple comparison test; N = 23–27, from 4 independent experiments).

3.3. Neurochemical Profile in the Brain of ACR-Injected Zebrafish Remains Unaltered

ACR exposure has been reported to induce changes in the neurotransmitters profile in the brain of different animal models. In contrast, when the profile of neurotransmitters was analyzed in the brain of control and ACR-injected fish, no changes were found in the levels of acetylcholine ($t(10)$ = 0.277 , P = 0.788), serotonin ($t(10)$ = -1.292 , P = 0.225), dopamine ($t(10)$ = -0.942, P = 0.369) or norepinephrine ($t(10)$ = -0.441, P = 0.668) (Supplementary Table S2). No differences were also found in the precursors of serotonin (tryptophan: $t(10)$ = 0.305 , P = 0.767 ; 5-HTP: $t(10)$ = -0.767, P = 0.461) and dopamine (tyrosine: $t(10)$ = -0.627 , P = 0.545; L-DOPA: $t(10)$ = -0.031 , P = 0.976) as well as in the degradation products of serotonin (5-HIAA: $t(10)$ = -1.794 , P = 0.103), dopamine (DOPAC: $t(10)$ = 0.394 , P = 0.704 ; 3-MT: $t(10)$ = 0.103 , P = 0.920; HVA: $t(10)$ =-0.356 , P = 0.729) and norepinephrine (normetanephrine: $t(10)$ = 1.299 , P = 0.223; epinephrine: $t(10)$ = 0.681 , P = 0.511).
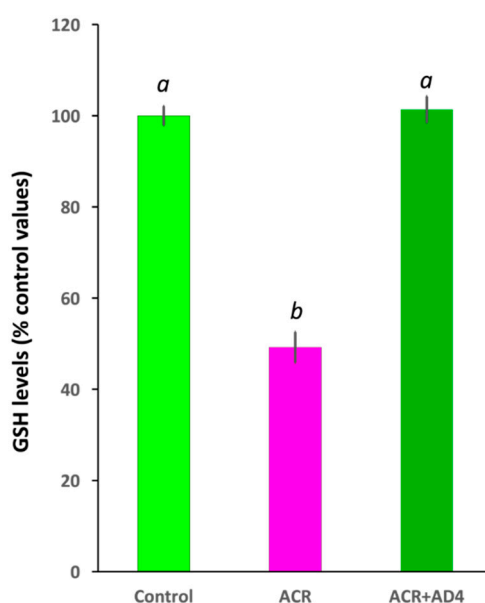

Figure 2. AD4 (single dose, 400 µg/g b.w., i.p.) administered 24 h after acrylamide exposure (single dose, ACR, 800 µg/g b.w., i.p) leads to full recovery of the reduced glutathione (GSH) levels in the adult zebrafish brain. Different letters indicate significant differences ($P < 0.05$) following one-way ANOVA (N: 23-33).

3.4. Lack of Differential Gene Expression in the Brain of ACR-Injected Zebrafish

Waterborne exposure to ACR has been reported to induce changes in the expression of genes related to redox homeostasis, synaptic vesicle recycling, regeneration, and myelination in the brain of adult zebrafish [8,9]. However, as shown in Supplementary Table S3, no significant differences were observed in the expression of 12 selected genes from these functional groups in the brain of zebrafish 48 hours after i.p. injection of ACR. Specifically, the expression levels of *nsf1a*, *syn2a*, *syt1a*, *syt2a*, *stxbp1b*, *gsr*, *gclc*, *txn*, *gap43*, *tubb5*, *gfap*, and *mbp* did not differ between control and ACR-injected fish.

3.5. ACR Delays Habituation to a Series of Acoustic Startle Stimuli and this Effect is Counteracted by AD4

In previous studies we demonstrated that waterborne exposure to ACR leads anxiety-like behavior in adult zebrafish [9,13]. However, we found that intraperitoneal injections lead relevant changes this type of behavior, suggesting that anxiety is not a suitable apical endpoint to be used in this study. Instead, in this work we have evaluated the effect of ACR on the sensitivity, habituation and prepulse inhibition of the acoustic startle response (ASR).

As shown in Table 1 and Supplementary Dataset 2, ACR-injection did not impair the main kinematic parameters of the ASR, including the latency, duration of the bending, amplitude of the C-bend, average angular velocity and maximal angular velocity of the ASR. Moreover, Supplementary Dataset 3 shows that no differences in sensitivity to the startle stimulus have been found between control ($20.00 \pm 4.16\%$ of responses) and ACR-injected ($22.22 \pm 3.51\%$ of responses) fish ($t(8) = -0.408$, $P = 0.694$). For the prehabituation step of the protocol, the frequency of responses for ACR treated fish (*Mdn* = 55.56%) showed a trend to decrease with respect to the corresponding controls (*Mdn* = 66.67%), and AD4 administration was not able to rescue this effect (*Mdn* = 55.56%). While the Kruskal-Wallis test revealed a statistically significant difference among the three groups ($H(2, 15) = 7.335$, $P = 0.026$), pairwise comparisons failed to identify significant differences among groups after correction for multiple comparisons (Control vs ACR, $P = 0.057$; Control vs ACR+AD4, P = 0.057; ACR vs ACR+AD4, $P = 1.00$).

Table 1. Kinematic parameters of the C-bend during the acoustic startle response in control and ACR-treated adult zebrafish.

Parameter	Control [Median, (IQR)]	Acrylamide [Median, (IQR)]	*U*	*z*	*P*
Latency (ms)	11 (10-12)	11 (10-12)	1729	0.347	0.729
Duration (ms)	12 (11-14)	11 (10-13)	1392	-1.556	0.120
Curvature (°)	99.3 (86.6-112.0)	102.5(77.5-115.8)	1696	0.147	0.883
Average Angular Velocity (°/ms)	8.4 (7.6-9.3)	8.8 (7.7-10.0)	1898	1.267	0.205
Maximal Angular Velocity (°/ms)	17.6 (15.5-19.7)	18.4 (16.2-20.9)	1906	1.311	0.190

U: Mann-Whitney U statistic; **z**: z-score.

Figure 3 shows that ACR injection delays habituation to the ASR and that this effect is fully recovered when AD4 was administered. The effect of ACR on the habituation process was analyzed by determining the % habituation during the initial (stimuli 1-5), middle (stimuli 6-10) and final (stimuli 11-15) periods of this neuromodulatory process (Supplementary Dataset 3). Figure 3 shows statistical differences between groups during the first 5 stimuli ($F(2,12) = 4.516$, $P = 0.036$), with a clear decrease in the % habituation in animals injected with ACR (*Mdn* = 20%) with respect to the corresponding controls (*Mdn* = 66.67%), and a full recovery of this parameter after the administration of AD4 (*Mdn* = 66.67%). A similar profile was found during the second period of habituation (stimuli 6-10; $H(2,15) = 8.519$, $P = 0.014$), with % habituation of 83.33%, 60.00% and 83.00% for the control,

ACR-injected and ACR+AD4 injected groups, respectively. Finally, during the last period of the habituation (stimuli 11-15), a similar trend was also observed, but this time the differences were not statistically significant ($H(2,15) = 2.559$, $P = 0.278$).

Finally, when % PPI (500 and 1000 ms as prepulse-to-pulse interval) of ASR was determined in adult zebrafish from the control, ACR, and ACR+AD4 groups, no statistically significant differences were found between control and ACR treated fish (Supplementary Dataset 4).

4. Discussion

In previous studies, we demonstrated that acute waterborne exposure to 0.75 mM ACR for 72h resulted in a 56% depletion of brain GSH levels (about 56%) in adult zebrafish, which was not rescued by N-acetylcysteine (NAC) due to its limited blood-brain barrier (BBB) permeability [9,13,14]. In this study, we developed a novel severe acute ACR neurotoxicity model using intraperitoneal (i.p.) injections to evaluate the therapeutic potential of NAC-amide (AD4), a BBB-permeable derivative of NAC [29]. However, administering the antidote via water exposure at concentrations ranging from 300 to 750 μM would require gram-scale amounts of the compound. While this approach is feasible for NAC due to its relatively low cost, NAC-amide is over 7,000 times more expensive, making this exposure route impractical. Therefore, the first step in this study was to develop a novel severe acute acrylamide-induced neurotoxicity model in adult zebrafish based on intraperitoneal injections. The results presented in this manuscript demonstrate that 48 hours after a single dose of 800 mg ACR/kg b.w., brain GSH levels decreased by approximately 51%, an effect comparable to the 56% reduction observed in the previous waterborne exposure model [9].
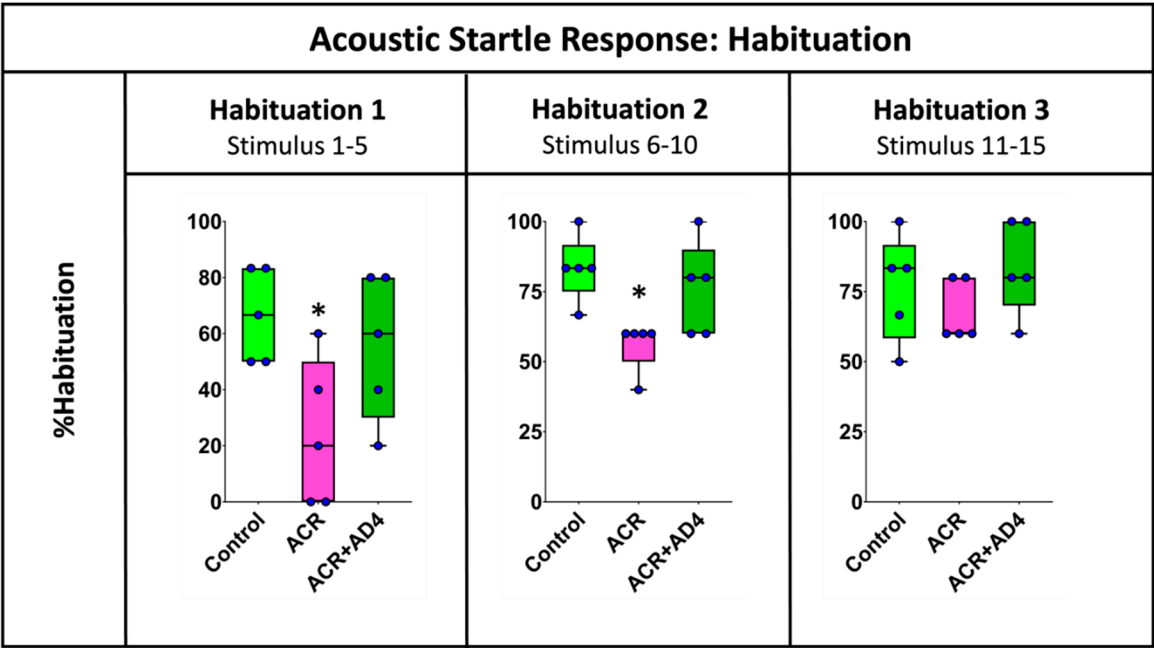

Figure 3. Analysis of the % habituation in adult zebrafish control, ACR and ACR+AD4 during the initial (stimuli 1-5), middle (stimuli 6-10) and final (stimuli 11-15) part of the habituation step (series of 15 startle stimuli with a 1 s interstimulus interval). Boxplot representation with the box indicating the 25th and 75th percentiles and the whiskers the maximum and minimum values. The thin line within the box marks the median. *$P < 0.05$ (N: 9 fish per experimental group, 15 reactions, in total, per fish).

The reported limitations of NAC in crossing the blood-brain barrier (BBB) [30] are clearly illustrated when comparing the recovery of brain GSH levels between NAC [14] and NAC-amide (AD4, this study) in animals acutely exposed to ACR. In the former study, animals were pretreated for 24 hours with two concentrations of NAC (equimolar and 0.4 times the ACR concentration) before being co-exposed to a mixture of 0.75 mM ACR and NAC at the same concentrations used for

pretreatment, for an additional 72 hours. In contrast, in the present study, NAC-amide (AD4) was not administered before or during ACR exposure but only once 24 hours after ACR administration. Additionally, the dose of AD4 was only 0.22 times the ACR dose. Remarkably, a full recovery of brain GSH levels was observed in this study with AD4, whereas no effect was found in the previous work with any concentration of NAC [14].

The disruption of synaptic vesicle recycling is a well-documented mechanism of ACR neurotoxicity, mediated by covalent modification of thiolate sites on proteins critical for synaptic function [31–33]. In our earlier work, waterborne ACR exposure altered the expression of genes involved in synaptic vesicle cycling (e.g., *nsf1a*, *syt1a*, *syn2a*, *stxbp1b*), redox homeostasis (e.g., *gsr*, *gclc*, *txn*), and regeneration (e.g., *gap43*, *gfap*, *tubb5*) in zebrafish brains [8,9,12]. However, in the current i.p. model, no significant changes were observed in the expression of these genes. This discrepancy may reflect differences in exposure paradigms: continuous waterborne exposure likely induces sustained cellular stress and transcriptional responses, whereas a single high-dose i.p. injection may cause rapid GSH depletion without triggering prolonged oxidative or neuroinflammatory signaling. Similarly, while waterborne ACR exposure altered neurotransmitter profiles in zebrafish brains [9], the i.p. model did not affect the levels of acetylcholine, serotonin, dopamine, or norepinephrine. These findings suggest that the toxicokinetics of ACR exposure plays a critical role in shaping its neurotoxic effects, as acute i.p. exposure primarily targets redox homeostasis without inducing broader transcriptional or neurochemical changes. Similarly to the observed effect at gene expression level, the discrepancy may stem from differences in toxicokinetics: continuous waterborne exposure likely induces sustained cellular stress, while a single high-dose intraperitoneal injection may cause rapid GSH depletion without triggering prolonged transcriptional or neurochemical responses [34]. Additionally, the resilience of neurotransmitter systems in our model could reflect compensatory mechanisms that maintain neurochemical balance under acute chemical stress conditions [35]. While these results suggest that neurotransmitter dynamics remain stable under the current exposure paradigm, further studies with finer temporal resolution or region-specific analyses are needed to fully rule out transient or localized effects.

Whereas acrylamide is primarily considered a neurotoxic compound affecting the peripheral nervous system, it also impacts the central nervous system, though research in this area remains limited [7]. In this study, we have analyzed the effect of the acute exposure to ACR on two neuroplasticity processes, short-term habituation and PPI of the ASR. The observed impairment in habituation may be linked to the reported effect of ACR on the synaptic vesicles recycling, a process critical for synaptic plasticity and neurotransmitter availability [36].

Granato et al., (2019) [37] identified five habituation regulatory modules in zebrafish, with Module 1 comprising of Huntingtin-interacting protein 14 (Hip14), NMDA receptors and dopamine receptors. Hip14 is a palmitoyl transferase that attaches palmitate to specific cysteine residues of synaptic proteins including receptors, channels, and proteins involved in synaptic vesicle dynamics [37]. By forming adducts with these cysteine residues, ACR could competitively inhibit palmitoylation, disrupting the trafficking and function of synaptic proteins. This mechanism provides a plausible explanation for the observed deficits in habituation, as palmitoylation is essential for synaptic plasticity. Furthermore, ACR's impairment of synaptic vesicle recycling could reduce the release of glutamate and dopamine into the synaptic cleft, diminishing the activation of NMDA and dopamine receptors. These disruptions would collectively contribute to the observed decrease in habituation.

The impairment in ASR short-term habituation observed in our study also aligns with previous reports linking GSH depletion to deficits in synaptic plasticity [38]. Animal models of schizophrenia and pharmacological GSH depletion (e.g., buthionine sulfoximine-treated rodents) have been shown to exhibit impaired synaptic plasticity and altered habituation responses [38,39]. Given that habituation is a form of non-associative learning requiring efficient synaptic adaptation, the observed deficits in our study may be attributed to oxidative stress-induced disruptions in neural circuits that mediate ASR modulation. Moreover, the fact that ACR did not significantly alter ASR kinematic

parameters or % PPI suggests that GSH depletion selectively disrupts neuroplasticity mechanisms underlying habituation without affecting the basic startle reflex or sensory gating processes, as recently reported in rodents [39].

Abbreviations

The following abbreviations are used in this manuscript:

AD4	N-acetylcysteine-amide
ACR	Acrylamide
ASR	Acoustic Startle Response
GSH	Reduced Glutathione
NAC	N-acetylcysteine

References

1. Park, R.M. Preliminary Risk assessment for Acrylamide and Peripheral Neuropathy. Neurotoxicology 2021, 85, 10–17, doi:10.1016/j.neuro.2021.04.004.
2. Kjuus, H.; Goffeng, L.O.; Heier, M.S.; Sjöholm, H.; Øvrebø, S.; Skaug, V.; Paulsson, B.; Törnqvist, M.; Brudal, S. Effects on the peripheral nervous system of tunnel workers exposed to acrylamide and N-methylolacrylamide. Scand. J. Work. Environ. Heal. 2004, 30, 21–29, doi:10.5271/sjweh.761.

3. Buyukdere, Y.; Akyol, A. From a toxin to an obesogen: a review of potential obesogenic roles of acrylamide with a mechanistic approach. Nutr. Rev. 2023, 82, 128–142, doi:10.1093/NUTRIT/NUAD041.

4. Bin-Jumah, M.; Abdel-Fattah, A.F.M.; Saied, E.M.; El-Seedi, H.R.; Abdel-Daim, M.M. Acrylamide-induced peripheral neuropathy: manifestations, mechanisms, and potential treatment modalities. Environ. Sci. Pollut. Res. 2021, 28, 13031–13046, doi:10.1007/S11356-020-12287-6/TABLES/1.

5. Li, L.; Li, J.; Luo, L.; Li, J.; Huang, H.; Xie, Y. Toxic encephalopathy, vision loss, and memory disorder caused by acute acrylamide exposure. J. Occup. Environ. Hyg. 2024, 21, 152–161, doi:10.1080/15459624.2024.2305135.

6. Kopańska, M.; Łagowska, A.; Kuduk, B.; Banaś-Ząbczyk, A. Acrylamide Neurotoxicity as a Possible Factor Responsible for Inflammation in the Cholinergic Nervous System. Int. J. Mol. Sci. 2022, Vol. 23, Page 2030 2022, 23, 2030, doi:10.3390/IJMS23042030.

7. Zhao, M.; Zhang, B.; Deng, L. The Mechanism of Acrylamide-Induced Neurotoxicity: Current Status and Future Perspectives. Front. Nutr. 2022, 9, 859189, doi:10.3389/FNUT.2022.859189/BIBTEX.

8. Raldúa, D.; Casado, M.; Prats, E.; Faria, M.; Puig-Castellví, F.; Pérez, Y.; Alfonso, I.; Hsu, C.-Y.; Arick II, M.A.; Garcia-Reyero, N.; et al. Targeting redox metabolism: the perfect storm induced by acrylamide poisoning in the brain. Sci. Rep. 2020, 10, 312, doi:10.1038/s41598-019-57142-y.

9. Faria, M.; Ziv, T.; Gómez-Canela, C.; Ben-Lulu, S.; Prats, E.; Novoa-Luna, K.A.; Admon, A.; Piña, B.; Tauler, R.; Gómez-Oliván, L.M.; et al. Acrylamide acute neurotoxicity in adult zebrafish. Sci. Rep. 2018, 8, doi:10.1038/S41598-018-26343-2.

10. Vorhees, C. V.; Williams, M.T.; Hawkey, A.B.; Levin, E.D. Translating Neurobehavioral Toxicity Across Species From Zebrafish to Rats to Humans: Implications for Risk Assessment. Front. Toxicol. 2021, 3, 629229, doi:10.3389/FTOX.2021.629229/BIBTEX.

11. Firdous, S.M.; Pal, S.; Khanam, S.; Zakir, F. Behavioral neuroscience in zebrafish: unravelling the complexity of brain-behavior relationships. Naunyn-Schmiedeberg's Arch. Pharmacol. 2024 39712 2024, 397, 9295–9313, doi:10.1007/S00210-024-03275-5.

12. Prats, E.; Gómez-Canela, C.; Ben-Lulu, S.; Ziv, T.; Padrós, F.; Tornero, D.; Garcia-Reyero, N.; Tauler, R.; Admon, A.; Raldúa, D. Modelling acrylamide acute neurotoxicity in zebrafish larvae. Sci. Rep. 2017, 7, doi:10.1038/s41598-017-14460-3.

13. Faria, M.; Valls, A.; Prats, E.; Bedrossiantz, J.; Orozco, M.; Porta, J.M.; Gómez-Oliván, L.M.; Raldúa, D. Further characterization of the zebrafish model of acrylamide acute neurotoxicity: gait abnormalities and oxidative stress. Sci. Rep. 2019, 9, 1–7, doi:10.1038/s41598-019-43647-z.

14. Faria, M.; Prats, E.; Gómez-Canela, C.; Hsu, C.-Y.; Arick, M.A.; Bedrossiantz, J.; Orozco, M.; Garcia-Reyero, N.; Ziv, T.; Ben-Lulu, S.; et al. Therapeutic potential of N-acetylcysteine in acrylamide acute neurotoxicity in adult zebrafish. Sci. Rep. 2019, 9, 16467, doi:10.1038/s41598-019-53154-w.

15. Costa, F. V.; Kolesnikova, T.O.; Galstyan, D.S.; Ilyin, N.P.; de Abreu, M.S.; Petersen, E. V.; Demin, K.A.; Yenkoyan, K.B.; Kalueff, A. V. Current State of Modeling Human Psychiatric Disorders Using Zebrafish. Int. J. Mol. Sci. 2023, 24, 3187, doi:10.3390/IJMS24043187/S1.

16. Martin, V.; Trus, M.; Atlas, D. Thiol-Based Redox Molecules: Potential Antidotes for Acrylamide Toxicity. Antioxidants 2024, 13, 1431, doi:10.3390/ANTIOX13121431/S1.

17. Pan, X.; Wu, X.; Yan, D.; Peng, C.; Rao, C.; Yan, H. Acrylamide-induced oxidative stress and inflammatory response are alleviated by N-acetylcysteine in PC12 cells: Involvement of the crosstalk between Nrf2 and NF-κB pathways regulated by MAPKs. Toxicol. Lett. 2018, 288, 55–64, doi:10.1016/J.TOXLET.2018.02.002.

18. Gilgun-Sherki, Y.; Barhum, Y.; Atlas, D.; Melamed, E.; Offen, D. Analysis of gene expression in MOG-induced experimental autoimmune encephalomyelitis after treatment with a novel brain-penetrating antioxidant. J. Mol. Neurosci. 2005, 27, 125–135, doi:10.1385/JMN:27:1:125/METRICS.

19. Atlas, D. Emerging therapeutic opportunities of novel thiol-amides, NAC-amide (AD4/NACA) and thioredoxin mimetics (TXM-Peptides) for neurodegenerative-related disorders. Free Radic. Biol. Med. 2021, 176, 120–141, doi:10.1016/J.FREERADBIOMED.2021.08.239.

20. Percie Du Sert, N.; Hurst, V.; Ahluwalia, A.; Alam, S.; Avey, M.T.; Baker, M.; Browne, W.J.; Clark, A.; Cuthill, I.C.; Dirnagl, U.; et al. The ARRIVE guidelines 2.0: Updated guidelines for reporting animal research. BMC Vet. Res. 2020, 16, 242, doi:10.1186/s12917-020-02451-y.

21. Stewart, A.; Cachat, J.M.; Suciu, C.; Hart, P.C.; Gaikwad, S.; Utterback, E.; Dileo, J.; Kalueff, A. V. Intraperitoneal injection as a method of psychotropic drug delivery in adult zebrafish. Neuromethods 2011, 51, 169–179, doi:10.1007/978-1-60761-953-6_14/FIGURES/14_3_192657_1_EN.

22. White, C.; Viernes, H.; Krejsa, C.; … D.B.-A.; 2003, undefined Fluorescence-based microtiter plate assay for glutamate–cysteine ligase activity. ElsevierCC White, H Viernes, C. Krejsa, D Botta, TJ KavanaghAnalytical Biochem. 2003•Elsevier.

23. Mayol-Cabré, M.; Prats, E.; Raldúa, D.; Gómez-Canela, C. Characterization of monoaminergic neurochemicals in the different brain regions of adult zebrafish. Sci. Total Environ. 2020, 141205, doi:10.1016/j.scitotenv.2020.141205.

24. Faria, M.; Bedrossiantz, J.; Ramírez, J.R.R.; Mayol, M.; García, G.H.; Bellot, M.; Prats, E.; Garcia-Reyero, N.; Gómez-Canela, C.; Gómez-Oliván, L.M.; et al. Glyphosate targets fish monoaminergic systems leading to oxidative stress and anxiety. Environ. Int. 2021, 146, 106253, doi:10.1016/j.envint.2020.106253.

25. Livak, K.J.; Schmittgen, T.D. Analysis of Relative Gene Expression Data Using Real-Time Quantitative PCR and the 2 C T Method. METHODS 2001, 25, 402–408, doi:10.1006/meth.2001.1262.

26. Stevanović, M.; Tagkalidou, N.; Multisanti, C.R.; Pujol, S.; Aljabasini, O.; Prats, E.; Faggio, C.; Porta, J.M.; Barata, C.; Raldúa, D. Zebra_K, a kinematic analysis automated platform for assessing sensitivity, habituation and prepulse inhibition of the acoustic startle response in adult zebrafish. Sci. Total Environ. 2025, 958, 178028, doi:10.1016/j.scitotenv.2024.178028.

27. Wolman, M.A.; Jain, R.A.; Liss, L.; Granato, M. Chemical modulation of memory formation in larval zebrafish. Proc. Natl. Acad. Sci. 2011, 108, 15468–15473.

28. Burgess, H.A.; Granato, M. Sensorimotor gating in larval zebrafish. J. Neurosci. 2007, 27, 4984–4994, doi:10.1523/JNEUROSCI.0615-07.2007.

29. Atlas, D.; Melamed, E.; Ofen, D. Brain Targeted low molecular weight hydrophobic antioxidant compounds. US Pat. USOO5874468A 1999.

30. Bavarsad Shahripour, R.; Harrigan, M.R.; Alexandrov, A. V. N-acetylcysteine (NAC) in neurological disorders: Mechanisms of action and therapeutic opportunities. Brain Behav. 2014, 4, 108–122, doi:10.1002/brb3.208.

31. LoPachin, R.M.; Gavin, T. Acrylamide-induced nerve terminal damage: Relevance to neurotoxic and neurodegenerative mechanisms. J. Agric. Food Chem. 2008, 56, 5994–6003, doi:10.1021/JF703745T/ASSET/IMAGES/LARGE/JF-2007-03745T_0001.JPEG.

32. LoPachin, R.M.; Barber, D.S. Synaptic Cysteine Sulfhydryl Groups as Targets of Electrophilic Neurotoxicants. Toxicol. Sci. 2006, 94, 240–255, doi:10.1093/TOXSCI/KFL066.

33. LoPachin, R.M.; Gavin, T.; Barber, D.S. Type-2 alkenes mediate synaptotoxicity in neurodegenerative diseases. Neurotoxicology 2008, 29, 871–882, doi:10.1016/J.NEURO.2008.04.016.

34. Exon, J.H. A Review of the Toxicology of Acrylamide. J. Toxicol. Environ. Heal. Part B 2006, 9, 397–412, doi:10.1080/10937400600681430.

35. Richendrfer, H.; Creton, R. Chlorpyrifos and malathion have opposite effects on behaviors and brain size that are not correlated to changes in AChE activity. Neurotoxicology 2015, 49, 50–58.

36. LoPachin, R.M.; Gavin, T. Molecular mechanism of acrylamide neurotoxicity: lessons learned from organic chemistry. Environ. Health Perspect. 2012, 120, 1650.

37. Nelson ID, J.C.; Shoenhard, H.; Granato, M.I.; Moens, C. Integration of cooperative and opposing molecular programs drives learning-associated behavioral plasticity. journals.plos.orgJC Nelson, H Shoenhard, M GranatoPLoS Genet. 2023•journals.plos.org 2023, 19, doi:10.1371/journal.pgen.1010650.

38. Kulak, A.; Steullet, P.; Cabungcal, J.H.; Werge, T.; Ingason, A.; Cuenod, M.; Do, K.Q. Redox dysregulation in the pathophysiology of schizophrenia and bipolar disorder: Insights from animal models. Antioxidants Redox Signal. 2013, 18, 1428–1443, doi:10.1089/ars.2012.4858.

39. Preissmann, D.; Dépré, M.; Schenk, F.; Gisquet-Verrier, P. Anxiety modulates cognitive deficits in a perinatal glutathione deficit animal model of schizophrenia. Brain Res. 2016, 1648, 459–468, doi:10.1016/j.brainres.2016.07.042.